Original Article

Comparative Histological Study on the Therapeutic Role of Bone Marrow derived Mesenchymal Stem Cells versus their Derived Exosomes on Experimentally Induced Liver Fibrosis in Adult Male Albino Rat

Alaa Mostafa Kassem, Sara Abd El Gawad El Sebay, Mohamed Abdelrahman Ahmed Mekawy and Heba M. Fawzy

Department of Histology, Faculty of Medicine, Ain Shams University, Egypt

ABSTRACT

Background: Liver fibrosis is a significant global health issue with limited treatment options, except for the elimination of the underlying cause or liver transplantation. Both bone marrow mesenchymal stem cells (BM-MSCs) and their exosomes (BM-MSC-EXOs) have demonstrated promise as therapeutic agents due to their ability to regenerate and immunomodulate.
Aim of the Work: To compare the therapeutic role of BM-MSCs and their exosomes on the liver's structure in adult male albino rats with carbon tetrachloride-induced liver fibrosis.
Material & Methods: Forty-five adult male albino rats were included in this study, 5 of them used to isolate MSCs. Group I (the control group) included ten rats. Group II included thirty rats that received CCl4 to induce liver fibrosis then subdivided equally into subgroup IIA (CCl4 group), subgroup IIB (BM-MSCs group) received BM-MSCs once and subgroup IIC (EXOs group) received EXOs once.
Results: CCl4 injection significantly induced hepatic dysfunction. It caused marked histological alternations, as confirmed by H&E, electron microscopy examination, and biochemical analysis of liver function. Rats treated with BM-MSCs, and exosomes showed considerable improvement in comparison with the CCl4-treated group. There was also a significant decrease in both the area percentages of collagen and TNF-α positive hepatocytes in these groups compared to CCl4-treated group. Although the rats treated by exosomes showed more improvement in all H&E, ultrastructure, and biochemical analysis, statistically there was a non-significant difference between BM-MSCs and exosome groups.
Conclusion: The study revealed that the therapeutic role of BM-MSCs-EXOs seemed to have a greater effect than the parent BM-MSCs in a rat model of liver fibrosis induced by CCl4.

Received: 15 January 2025, **Accepted:** 12 February 2025

Key Words: BM-MSCs; CCL4; exosomes; liver fibrosis; TNF-α.

Corresponding Author: Heba M. Fawzy, MD, Department of Histology, Faculty of Medicine, Ain Shams University, Egypt, **Tel.**: +20 12 2400 3152, **E-mail:** hebafawzy@med.asu.edu.eg

ISSN: 1110-0559, Vol. 48, No. 2

INTRODUCTION

Liver fibrosis involves excessive extracellular matrix deposition, hepatocyte damage, and altered vascular architecture, primarily caused by chronic liver inflammation from factors like viral infections, alcohol, non-alcoholic steatohepatitis, autoimmune conditions, or hereditary diseases[1,2]. If untreated, it can progress to cirrhosis or hepatocellular carcinoma[3], with symptoms often unnoticed until advanced stages[4]. Fibrosis progresses from mild to severe, with complications like portal hypertension[5]. Reversing liver fibrosis is possible by treating the underlying cause and shifting immune responses toward repair[6].

Carbon tetrachloride (CCl4) is a toxic, mutagenic, and environmentally persistent halogenated hydrocarbon compound, commonly used in industrial processes like chlorofluorocarbons production, insecticides, petroleum refining, and as a solvent in fat, oils, and rubber processing[7,8]. It is a colorless, volatile compound that has a long half-life of 30-100 years in the atmosphere due to its great chemical stability[9]. CCl4 is primarily toxic to the liver but also affects the kidneys, lungs, spleen, and other tissues. It is absorbed via the skin, gastrointestinal tract, and respiratory system, with up to 60% absorption through respiration in humans. Fat and alcohol consumption can increase its absorption[10]. Known for its carcinogenic properties, CCl4 induces liver damage through oxidative stress, making it a widely used model to induce liver fibrosis[11].

BM-MSCs are multipotent cells that can differentiate in multiple directions and have pro-angiogenic and immunomodulatory properties. They express CD105, CD73, and CD90, but are negative for CD45 and CD34, making them less immunogenic than embryonic stem cells[12,13]. BM-MSCs are recognized for their potential role in treating liver fibrosis due to their ability to regulate immune cells and reduce inflammation[14].

DOI: 10.21608/ejh.2025.351566.2194

Exosomes are extracellular vesicles with a diameter of 30 to 150 nm, they transfer lipids, RNA, and proteins, to facilitate intercellular communication and affect cellular functions[15,16]. Exosomes, which are derived from multivesicular bodies, include proteins, lipids, and nucleic acids including mRNAs and miRNAs. Their function is determined by their selective packing[17]. MSC-EXOs are effective in treating liver diseases by reducing inflammation, fibrosis, and promoting regeneration. MSC-EXOs are a promising treatment option for liver diseases since they are smaller, easier to store compared to MSCs, and can target the liver specifically when given intravenously[18].

The liver can regenerate after injury, supported by autocrine, paracrine, and endocrine signaling pathways. Regeneration is proportional to the severity of the injury, with different processes triggered depending on the extent of liver damage[19,20].

MATERIALS AND METHODS

Animals

The study included 45 male albino Wistar rats. Five young male albino rats weighing 80-90 g and aged around one month were used for the isolation of MSCs. Forty adult rats weighing 150-200 gm body weight and about eight weeks were used. Throughout the experiment, the rats lived in hygienic plastic cages covered with mesh wire and had unrestricted access to tap water and an ordinary rat chow diet. The proper amount of light, temperature, and humidity were maintained for them. The examination was carried out at the Medical Research Centre in Ain Shams University, Faculty of Medicine (MASRI). It was carried out in compliance with the rules established by the US Office for Human Research Protections, the US Code of Federal Regulations, the International Council on Harmonization (ICH), and the Islamic Organization for Medical Science (IOMS). Federal Wide Assurance No. FWA 00017585 covers this study.

Experimental animal models

Following 7 days acclimatization, the rats were classified into 2 groups. Ten weeks after the experiment began, all the rats were sacrificed. The control group included ten rats without any interference till the end of the experiment. Multiple doses of 3 ml/kg body weight of 30% CCl4 (Advent, India, F22D049) in olive oil were delivered intraperitoneally to thirty rats from subgroups IIA, IIB, and IIC two times per week for eight weeks to induce liver fibrosis[21]. After eight weeks, rats of subgroup IIA (ten rats) left without any interference. On the first day of week nine, subgroup IIB (BM-MSCs group)[22] (consisted of ten rats), each rat received 1×10^6 MSCs in 150µL PBS once through the tail vein and then was sacrificed at the end of week ten. Subgroup IIC (EXOs group)[21] formed of ten rats, each rat received 158 µg EXOs (gathered from 1×10^6 MSCs) in 150µL PBS once in the tail vein on the first day of week nine and then was sacrificed at the end of week ten.

Cell culture

The study details a method for the culture of MSCs from the bone marrow of albino rats, guided by Drommelschmidt *et al*.[23]. Bone marrow was obtained from the femurs and tibiae of anesthetized rats, which were sterilized, dissected, and transported to the lab. In a sterile environment, the marrow was flushed from the bones, dissociated, and centrifuged. Cells were suspended in a complete culture medium composed of DMEM, FBS, sodium bicarbonate, and a penicillin-streptomycin solution (IG technology company, Giza, Egypt), then incubated with 5% CO_2 at 37°C. Cells that didn`t adhere were eliminated after 24 hrs, and every 3 days the medium was changed. Trypan blue and a hemocytometer were used to measure the number and vitality of cells[24].

To characterize MSCs, cells were immune stained for CD markers (CD45, CD44, and CD73) and analyzed by flow cytometry (Figure 1a), following protocols outlined by Zhang *et al*.[25] and Chu *et al*.[26]. Before staining, cells were blocked with 3% BSA to avoid non-specific binding, followed by a 30-minute dark incubation period with antibodies at 37°C. Fluorescence was evaluated using a FACScaliber flow cytometer, and data was analyzed with Flow Jo software. This approach allowed for the successful isolation, culture, and validation of MSCs, providing a controlled method to yield viable stem cells for further studies.

Exosomes isolation and quantification

Once MSC cultures reached 80–90% confluency, the cells were cultivated for 48 hours in a serum-free medium after being washed with PBS to allow exosome release. Exosome isolation was conducted through a multi-step ultracentrifugation process[27] at the National Research Center in Cairo. After initial low-speed centrifugations to remove cells and debris, the samples underwent high-speed ultracentrifugation at 100,000 x g, yielding a pellet of small extracellular vesicles, which was resuspended in PBS.

Characterization of exosomes was performed with transmission electron microscopy (TEM) at the Regional Center for Mycology and Biotechnology, Al-Azhar University. The exosomes were observed under a JEOL-1010 microscope, where they had a mean diameter of approximately 65.238 nm[22] (Figures 1b,c). Exosomes were quantified by BCA (bicinchoninic acid) protein assay at Nawah Scientific in Cairo. This colorimetric method measured protein concentration by assessing absorbance at 562 nm, a value directly correlated to protein content, following the principles outlined by Goldring[28] and Habibian *et al*.[29].

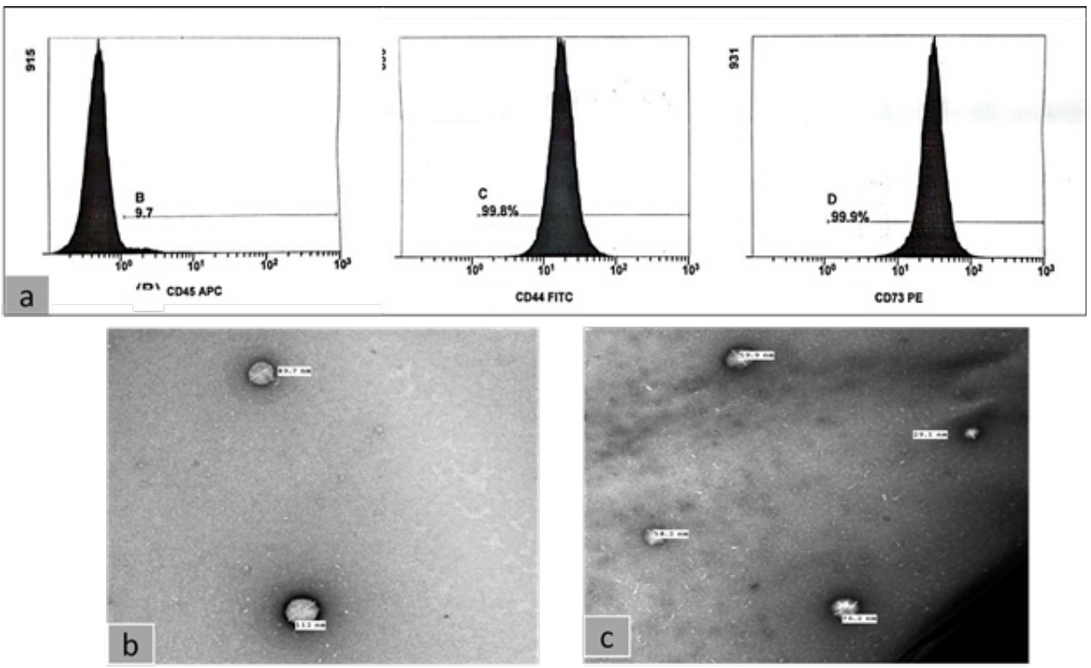

Fig. 1: Stem Cell & exosomes characterization: (a) Flow cytometry for BM-MSCs indicates (-ve) expression for CD45 and (+ve) expression for CD44 and CD73. (b)&(C) Characterization of exosomes by TEM (X100000).

Sample collection and preparation of tissues

After the experiment was over, 40 mg/kg body weight of thiopental sodium phosphate intraperitoneally delivered to rats[30] and were sacrificed by cervical dislocation. Through an anterior abdominal incision, the livers were cut aside, and blood was taken via the jugular vein. The right lobes of livers were collected from all animals. They were promptly put in ten percent formalin over five days for fixation, then they were dehydrated in an ascending alcohol grade, cleared by xylene, and then paraffin was used for embedding. five µm thickness sections were cut serially and then stained with Hematoxylin and Eosin stain (H&E) and Masson′s trichrome stain to detect collagen fibers.

On paraffin-embedded slices, we used the avidin-biotin complex immunoperoxidase technique to identify TNF-α[31]. Sections were put in xylene for one hour for deparaffinization. They were hydrated in decreasing concentrations of alcohol and then rinsed in distilled water. They were put in a hydrogen peroxide block for five minutes. Sections were rinsed with distilled water 3 times for 5 minutes each in PBS after all next steps. Antigen retrieval was carried out at 90C° in a microwave for 3 minutes then incubated with hydrogen peroxide for 20 minutes and blocked with Ultra V Block for 8 minutes to block nonspecific background staining. After draining, primary TNF-α antibody (100 µg/ml of Rabbit polyclonal IgG, 1:50 dilution; Santa Cruz Biotechnology, Inc., Dallas, TX, USA (cat# sc1350) were used, and sections were incubated at 4C overnight. The secondary antibody (Histostain-Plus Kit, In*vitro*gen, Carlsbad, CA, USA.) was applied for 20 minutes. Streptavidin peroxidase was applied for 20 minutes. Sections were washed with PBS, and DAB was used for 10 minutes. Harris's hematoxylin was used as Counterstain for 45 seconds, dehydrated by ascending grades of alcohol, cleared by xylene, and mounted by DPX. The main antibody was substituted with PBS for the negative controls.

For microscopic inspection, a microscope (Leica, DM2500) was utilized, with a Canon EOS 1100D Digital SLR camera, with the magnification set to 10 (ocular) x 10 and 40 (object lens).

Histomorphometric Study and statistical analysis

The measurements were estimated using the ImageJ[21]. Measurements were obtained from 3 distinct slides per rat across all groups. From each slide, five independent fields (non-overlapped fields) were carefully examined to find the mean area % of collagen and TNF-α immune reaction.

Every study's morphometric data was gathered and then statistically examined. The Statistical Package for the Social Sciences (SPSS) statistical tool class 21 (IBM Inc., Chicago, Illinois, USA) was utilized for the determination of the standard deviation (SD) and the mean of the measured parameters in each group. Comparison between studied groups was done using One-way analysis of variance (ANOVA). LSD post-hoc test was done to detect significance between groups. Values were shown as mean and SD. The significance was detected by probability of chance (*P- value*) where; *P value* < 0.05 (significant) and *p*>0.05 (non-significant).

Biochemical assessment

Samples of blood were centrifuged after clotted at room temperature for twenty minutes at 3000 rpm., then kept between -18 and -20 OC[32]. Biochemical analyses were performed in Leptovet lab, Cairo.

The following parameters were investigated: AST, ALT, Total Bilirubin, Direct Bilirubin, and Albumin. The lab assessed them utilizing test kits acquired from Roche Diagnostic Ltd (Germany).

RESULTS

Histological and immunohistochemical results

We recorded 2 deaths in subgroup IIA, one death in subgroup IIB and IIC, and no deaths in the control group.

On a gross level, the livers of the CCl4-treated group were large, hard, and had a fibrous capsule. The livers of the BM-MSCs and exosomes treated groups were fiery red softer, and glossier than those of the diseased group.

Histological findings

Hematoxylin and eosin staining

Control group I: The histological examination of liver sections of Group I (control rats) revealed normal liver architecture, with ill-defined hepatic lobules composed of radiating and anastomosing hepatocyte cords arising from the central vein and blood sinusoids in between. At the corners of the hepatic lobules were the interlobular portal regions, which housed bile ductules lined by cuboidal epithelium, hepatic artery, and portal vein, flat endothelial cells lined both (Figure 2a). The hepatocytes appeared polygonal with acidophilic granular cytoplasm, single vesicular nuclei with some binucleated cells, and prominent nucleoli. The blood sinusoids lined by Kupffer cells with rounded nuclei and flat endothelial cells lined (Figure 2b).

CCl4-treated (Subgroup IIA): Liver sections of subgroup IIA that injected with CCL4 injections for 8 weeks showed marked distortion in liver parenchyma. The cytoplasm of the majority of the hepatocytes seemed to be vacuolated (Figure 3a). The nuclei of certain vacuolated hepatocytes were darkly stained, distorted, and shrunken (Figure 3b). There were mononuclear cellular infiltrations near the congested and dilated portal vein. There was bile ductule proliferation (Figure 3c).

BM-MSCs-treated (Subgroup IIB): Liver sections of subgroup IIB revealed moderate improvement in both the stroma and parenchyma of the liver. Most of liver lobules were nearly comparable to control group (Figure 4a). Most hepatocytes had slightly vacuolated cytoplasm and central rounded vesicular nuclei. There was mild mononuclear cellular infiltration around the portal area and central veins (Figure 4b). There were still some areas with congested portal veins, central veins, and blood sinusoids.

Exosomes-treated (Subgroup IIC): Liver sections of subgroup IIC showed apparent improvement in the liver architecture. Almost all liver lobules were nearly comparable to control group (Figure 4c). Hepatocytes arranged in radiating and anastomosing cords arising from the central vein and portal tracts were seen at the corners. Although there was a small area of inflammatory cellular infiltration in a few fields. Hepatocytes` cytoplasm was acidophilic and granular with vesicular nuclei (some binucleated) and hepatic blood sinusoids in between (Figure 4d).

Masson trichrome-stain

Liver sections of control group revealed thin, green-colored collagen fibers surrounding the central vein (Figure 5a). While sections from the CCl4 group revealed an obvious increase in green-colored collagen fibers surrounding the central vein with collagen fibers between and surrounding the hepatocytes (perisinusoidal fibrosis) (Figure 5b). On contrast, sections from the BM-MSCs group appeared with few collagen fibers surrounding the central vein and in the perisinusoidal space (Figure 5c). Sections of the liver of the EXOs group also appeared with few collagen fibers around the central vein and in between the hepatocytes (Figure 5d).

Anti-TNF-α immuno-histochemical results

Liver sections of the control group showed negative cytoplasmic immune reaction within hepatocytes (Figure 6a). Although CCl4 group showed a strong positive brown cytoplasmic reaction in most hepatocytes (Figure 6b). Liver sections of BM-MSCs group revealed some cells with strong positive brown cytoplasmic reaction (Figure 6c). While liver sections of EXOs group revealed hepatocytes with negative cytoplasmic reaction in almost all fields (Figure 6d).

Electron microscope results

Liver sections of the control group showed normal hepatocytes with euchromatic central, rounded nuclei, with some binucleated cells. The cytoplasm has numerous mitochondria, lysosomes, rER, and scattered rosettes of glycogen granules (Figure 7a). Bile canaliculi were observed in between hepatocytes, with stunt microvilli projecting into their lumina and junctional complexes attaching neighboring cells (Figure 7b). Kupffer cells with phagocytic vesicles and endothelial cells with flattened nuclei lined the blood sinusoids. The perisinusoidal space showed microvilli from hepatocytes and contained HSCs with elongated nuclei and cytoplasmic lipid droplets (Figure 7c).

On contrast, liver ultra-thin sections of the CCl4 group revealed hepatocytes with irregularly shrunken nuclei, vacuolated cytoplasm, and small, well-defined lipid droplets of different diameters. Comparing to control group, there was an evident reduction in the amount of glycogen, as well as an apparent decrease in the mitochondria, which

appeared elongated and deformed, and a rough endoplasmic reticulum with dilated cisternae (Figure 8a). Collagen fibrils were observed between hepatocytes (Figure 8b), while blood sinusoids were dilated and lined by Kupffer cells with phagocytic vesicles (Figure 8c). Additionally, microvilli in perisinusoidal were disrupted, and there were transformed hepatic stellate cells (myofibroblast) (Figure 8d).

While ultrathin sections of the BM-MSCs group revealed hepatocytes containing euchromatic nuclei with vacuolated cytoplasm nearly comparable to the control group. Also, hepatocytes revealed mitochondria with a relatively normal appearance of their cristae alongside rER and lysosomes (Figure 9a). Bile canaliculi contained short microvilli protruding into their lumen. Neighboring hepatocytes were attached to each other by junctional complexes near the canaliculus (Figure 9b). Microvilli in perisinusoidal space were nearly like those of the control group. Kupffer cells lined the blood sinusoids (Figure 9c). Ultrathin sections of the EXOs group showed restoration of hepatocyte histological pattern near normal in most sections (Figures 9d,e).

Biochemical analysis

Statistically, the mean of ALT, AST, total bilirubin, and direct bilirubin showed that subgroup IIA had a significant increase comparing by the control group. In comparison with control group the mean level of Albumin was significantly decreased in subgroup IIA. Both subgroups IIB and IIC showed nonsignificant differences compared to control group. Both groups III and IV showed a significant decrease in ALT, AST, total bilirubin, and direct bilirubin and a significant increase in albumin level in comparison with subgroup IIA. By comparing subgroups IIB and IIC, there were non-significant differences between them, although subgroup IIC showed better improvement than subgroup IIB (Table 1, Histogram 1).

Statistically, the mean area percentage of collagen fibers and TNF-α immune reaction showed that subgroup IIA (CCl4 group) had a significant increase in comparison with control group. Both subgroups IIB and IIC showed non-significant difference in comparison with control group. Both subgroups IIB and IIC showed a significant decrease compared to subgroup IIA. By comparing subgroups IIB and IIC, there was a non-significant difference between them, but subgroup IIC showed better improvement than subgroup IIB (Table 1, histogram 1).

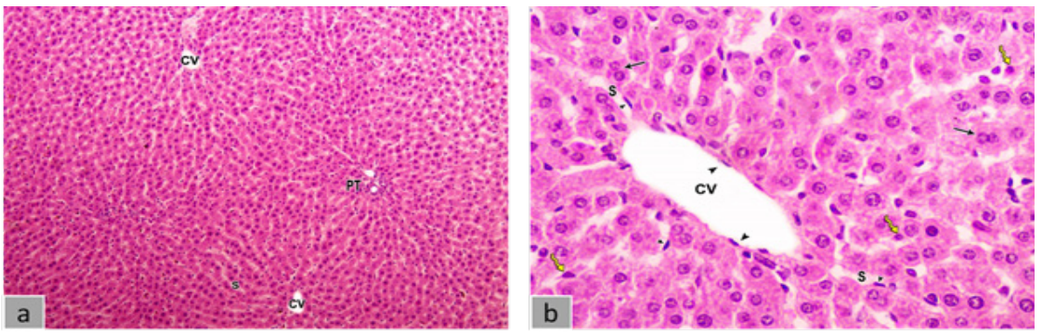

Fig.2: Liver sections of control group: (a) normal hepatic pattern with central vein (CV) in the center of lobules and portal tract (PT) at the periphery (H&E, X100). (b) Hepatocytes are present in anastomosing cords, some of them are binucleated (black arrow) (H&E, X400). Blood sinusoids (S). Kupffer cell (yellow arrow), endothelial cell (arrowhead).

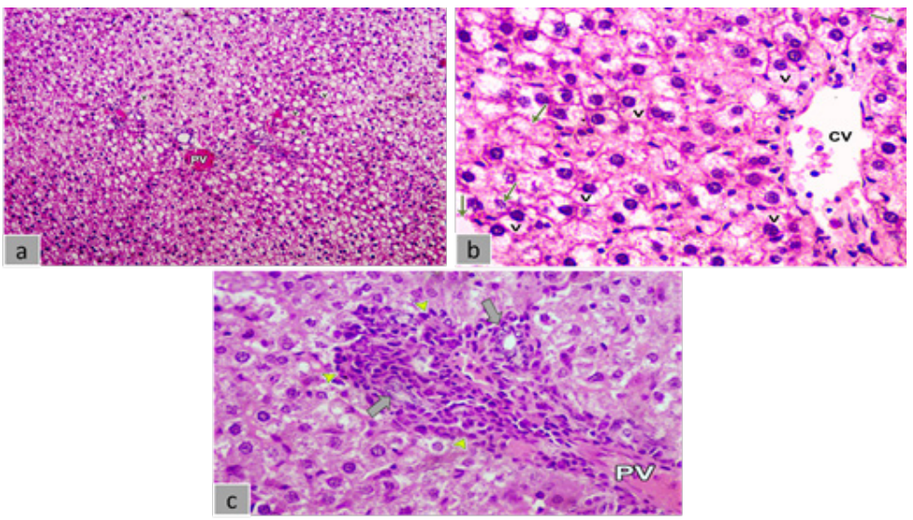

Fig. 3: Liver sections of subgroup IIA: (a) distorted liver pattern with a congested portal vein (PV) (H&E, X100). (b) Hepatocytes showing vacuolations (V) and some cells with shrunken nuclei (green arrow) (H&E, X400). (c) Mononuclear cellular infiltrations appear in the portal area (yellow arrowhead) with dilated portal vein (PV), ductular proliferation (grey arrow) (H&E, X400).

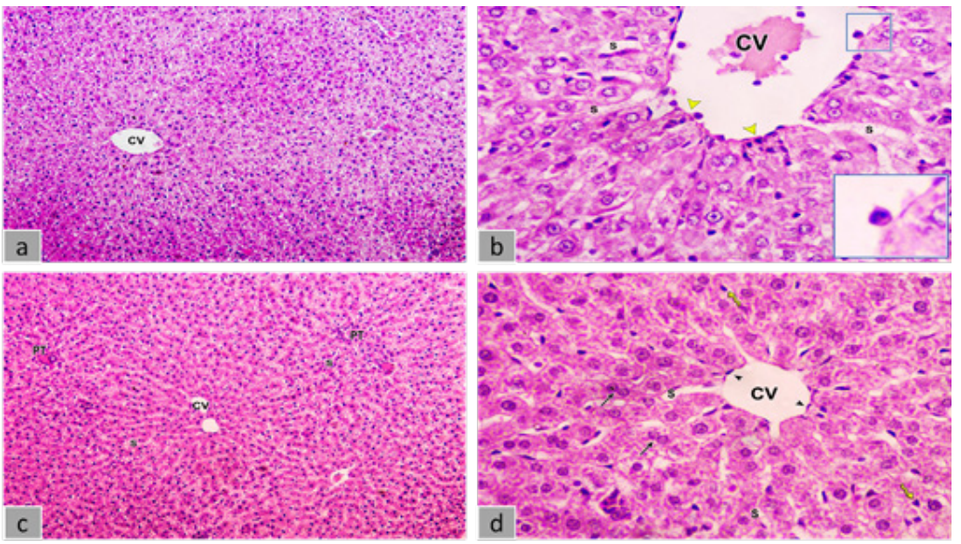

Fig. 4: Liver sections of BM-MSCs group (a & b): (a) nearly normal hepatic architecture (H&E, X100). (b) Slightly vacuolated cytoplasm with some of inflammatory cellular infiltration (yellow arrowhead) (H&E, X400) The inset Showing neutrophil (H&E, X1000). (c) sections of the liver of EXOs group (c & d): (c) normal hepatic lobules (H&E, X100). (d) Hepatocytes appeared with granular acidophilic cytoplasm, binucleated cells (black arrow) and separated by hepatic blood sinusoids (s) lined by endothelial cells (arrowhead) and Kupffer cell (yellow arrow) (H&E, X400).

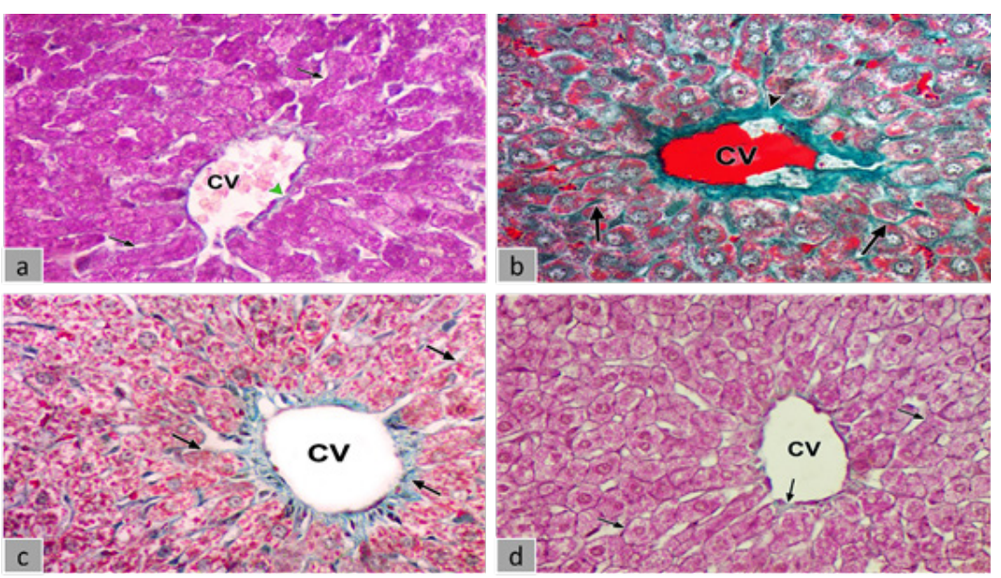

Fig. 5: (a) Masson trichrome-stained liver section of control group with thin, green-colored collagen fibers around the central vein (green arrow). (b) liver sections of subgroup IIA with thick collagen fibers surrounding the central vein (black arrowhead) and perisinusoidal fibrosis (black arrow) was seen. (c) Sections of the liver of subgroup IIB with few perisinusoidal fibrosis. (d) liver sections of subgroup IIC with few collagen fibers surrounding the central vein (black arrow). (Masson trichrome, X400)

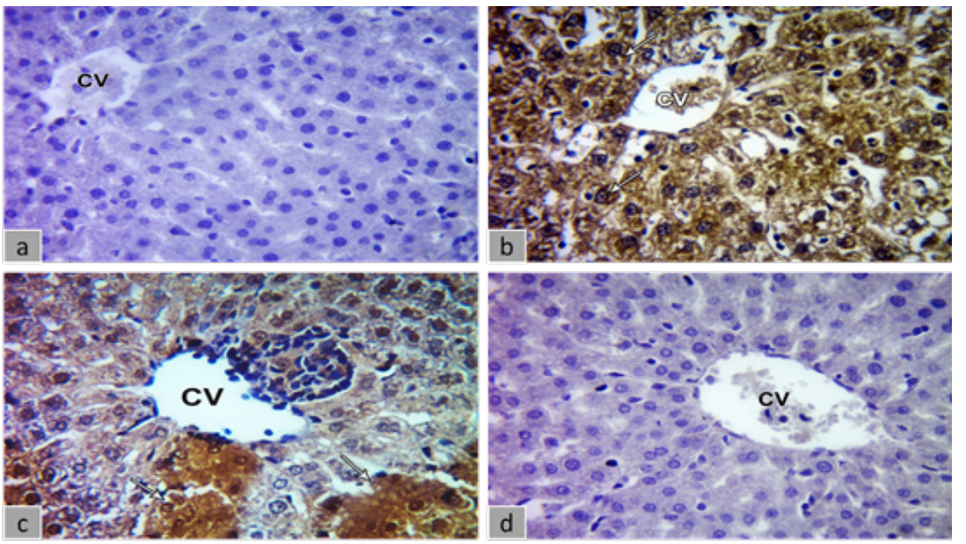

Fig. 6: (a) Liver sections of the control group with negative TNF-α cytoplasmic reaction. (b) Liver sections of subgroup IIA with strong cytoplasmic reaction. (c) Liver sections of subgroup IIB revealed some cells with strong cytoplasmic reaction (white arrow). (d) Liver sections of subgroup IIC with negative cytoplasmic reaction. (Immunostaining for TNF-α, X400)

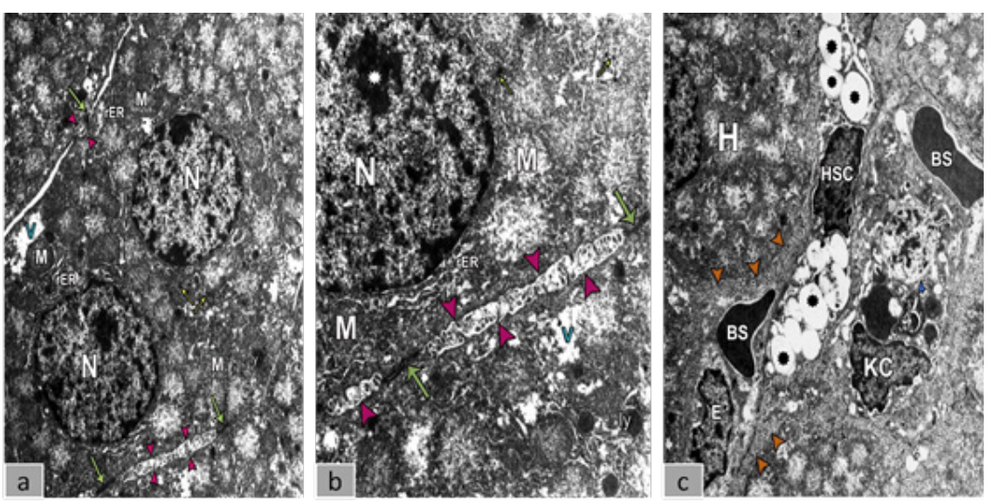

Fig. 7: TEM micrograph of liver sections of the control group revealing (a) binucleated (N) hepatocyte has many mitochondria (M), (rER), and glycogen granules (yellow arrow) (TEM X6000). (b) Normal bile canaliculi (violet arrowhead) and junctional complex (green arrow) (TEM X1200). (c) Blood sinusoid (BS) with normal microvilli (orang arrowhead), Kupffer cell (KC), and hepatic stellate cell (HSC) with lipid droplets (black asterisk) (TEM X6000).

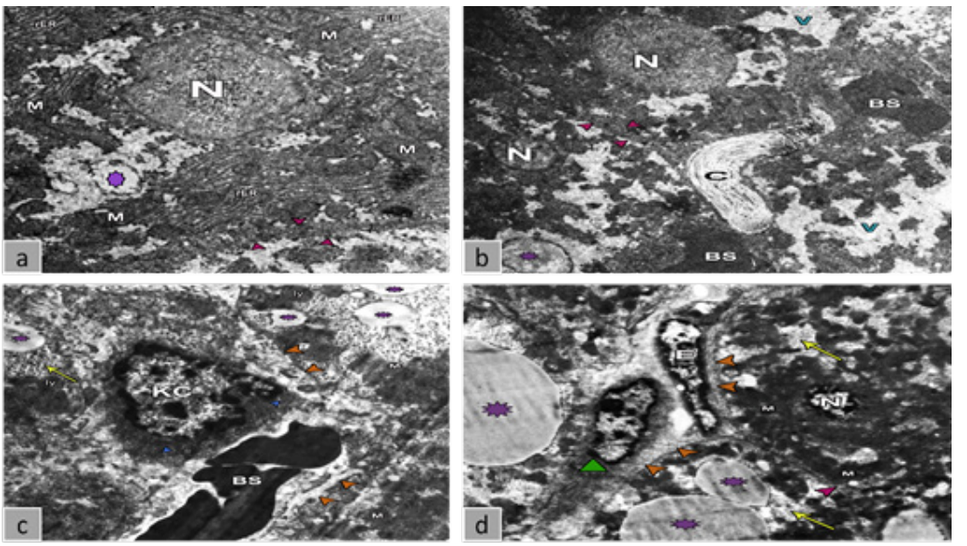

Fig. 8: TEM micrograph of liver sections of CCl4 group revealing (a) Hepatocytes with shrunken irregular nucleus (N) with lipid droplets (violet asterisk) and dilated (rER) (TEM X10000). (b) Hepatocyte with shrunken nucleus (N) contained lipid droplet (violet asterisk) with disturbed bile canaliculi (violet arrowhead) and collagen fibrils (C) between hepatocytes and blood sinusoids (BS) (TEM X6000). (c) Congested blood sinusoid (BS), Kupffer cell (KC), and disrupted microvilli (orang arrowhead) (TEM X12000). (d) Lipid droplets in hepatocyte (violet asterisk) and (myofibroblast) (green triangle) in perisinusoidal (TEM X6000).

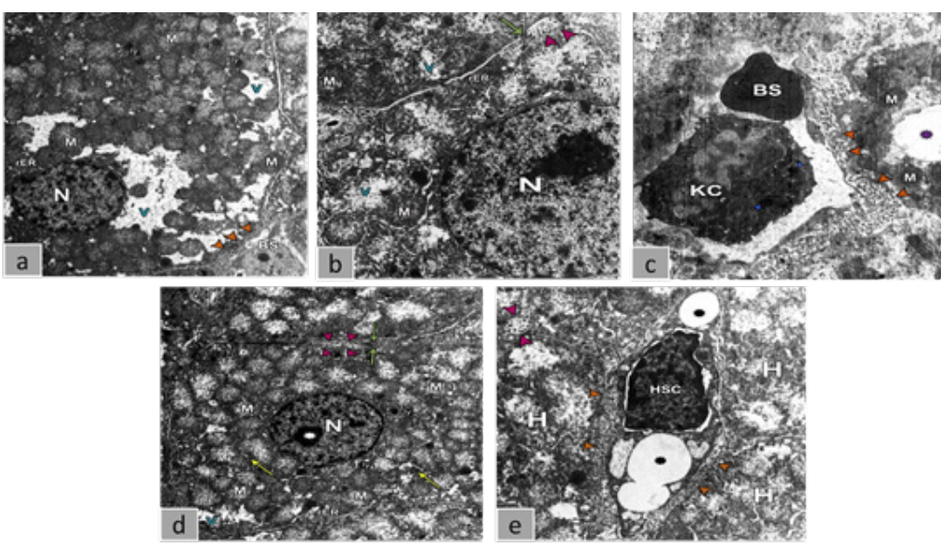

Fig. 9: TEM micrograph of liver sections from subgroup IIB (a, b & c) showing (a) Hepatocyte contain abundant mitochondria (M) and some vacuolations (V) (TEM X6000). (b) Bile canaliculi showed near normal microvilli (violet arrowhead) and junctional complex (green arrow) (TEM x12000). (c) Blood sinusoid lined by Kupffer cell (KC) and microvilli (orang arrowhead) (TEM X10000). Liver sections from subgroup IIC (d & e) showing (d) Hepatocyte comparable to the control group (TEM X6000). (e) Hepatic stellate cell (HSC) with lipid droplets (black asterisk) (TEM X12000).

Table 1: Statistical analysis in the form of the mean ± SD of study groups

Parameters	Group I	Subgroup IIA	Subgroup IIB	Subgroup IIC
Mean area % of collagen fibers	10.5±2.1	37.6±4.4	12.1±1.8	11.4±1.8
Mean area of TNF-α immune reaction	0.006±0.002	23.4±8.34	0.97±0.8	0.86±0.6
Mean level of ALT	37.7±2.3	147±14.1	45.1±5.6	44.8±6.3
Mean level of AST	49.1±6.2	296.9±12.8	55±8.5	52.1±5.3
Mean level of Total bilirubin	0.14±0.08	2.7±0.35	0.18±0.08	0.17±0.07
Mean level of Direct bilirubin	0.05±0.03	0.9±0.12	0.06±0.03	0.05±0.02
Mean level of Albumin	3.3±0.3	1.9±0.2	3.1±0.14	3.2±0.11

TNF-α: tumor necrosis factor-alpha, ALT: Alanine aminotransferase, AST: Aspartate aminotransferase

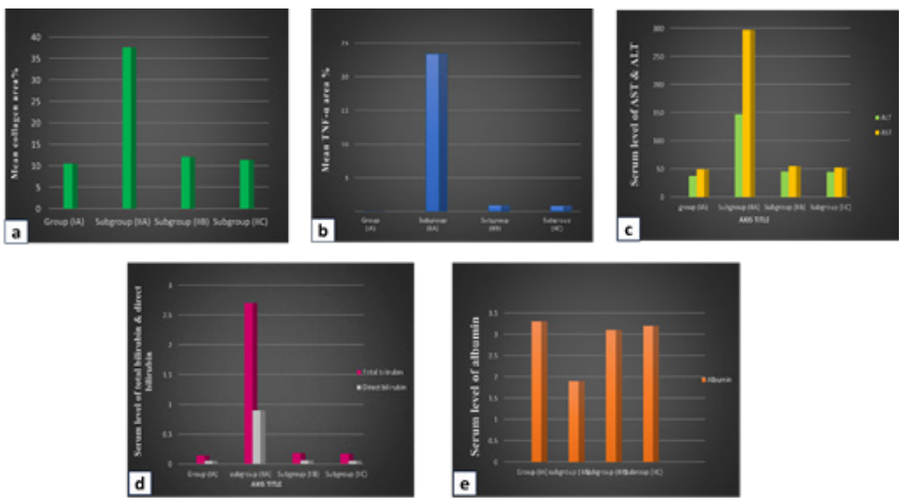

Histogram 1: Morphometric study of (a) mean area % of collagen fibers, (b) mean area % of TNF-α immune reaction, (c) biochemical analysis of ALT & AST, (d) biochemical analysis of Total bilirubin & Direct bilirubin, (e) biochemical analysis of Albumin.

DISCUSSION

The liver, as the body's largest digestive gland, is vulnerable to substances like alcohol, lipids, drugs, and poisons such as carbon tetrachloride (CCl4), which can cause acute and chronic damage, leading to hepatic fibrosis[33]. This study`s objective was to estimate the effects of BM-MSCs and their exosomes on liver architecture in rats with hepatic fibrosis induced by CCl4. In the recent study, we have revealed that BM-MSCs and their derived exosomes can alleviate liver fibrosis. Moreover, the therapeutic effect of BM-MSCs-EXOs seemed to be greater than the effect of their parent cells.

Histological examination of CCl4-treated rats (Subgroup IIA) showed marked liver distortion, in which almost all hepatic lobules were apparently affected, hepatocyte vacuolization, and inflammatory cell infiltration, consistent with findings by Wang *et al*., Wu *et al*., and Zein *et al*.[1,34,35]. Transmission electron microscopy revealed hepatocyte losing its normal histological pattern appearing with pyknotic nucleus with mitochondrial swelling, alongside myofibroblast transformation of HSC[35,36]. CCl4-induced liver fibrosis is driven by oxidative stress, where CCl4 metabolites cause lipid peroxidation and hepatocyte apoptosis[11,37], and activate Kupffer cells, which release cytokines promoting cell death[38].

Biochemical analysis showed increased ALT, AST, total bilirubin, and direct bilirubin levels, and reduced albumin levels in CCl4-treated rats, reflecting liver dysfunction. These results align with Unsal *et al*., Zein *et al*., and Salem *et al*.[9,35,38], highlighting the severity of liver damage. Elevated ALT and AST levels reflect hepatocyte injury, while elevated bilirubin indicates membrane damage, and decreased albumin levels suggest liver dysfunction[11].

Salem *et al*., explained that damaged and apoptotic hepatocytes trigger HSC trans-differentiation into myofibroblasts via several convergent pathways can damage the normal extracellular matrix of the perisinusoidal space, attract immune cells, and generate reactive oxygen species (ROS) and other fibrogenic and proinflammatory substances[38].

Tissue fibrosis in CCL4-treated rats resulted from Pro-inflammatory mediators and oxidative stress which affect the behavior of myofibroblasts by upregulating profibrogenic genes, including procollagen type I and tissue inhibitor of metalloproteinase-1[38,39]. CCl4 activated proinflammatory cytokine-producing Kupffer cells and significantly upregulated the expressions of TNF-α[9]. This finding agrees with our results.

Hao *et al*. added that HSC transdifferentiating into myofibroblast is stimulated by damaged and apoptotic hepatocytes through several converging pathways, which initiate and maintain the activation of HSCs by recruitment of immune cells, the release of reactive oxygen species (ROS) and other fibrogenic/ proinflammatory mediators, and disruption of the normal ECM of the space of Disse[40].

Masson trichrome staining confirmed fibrosis, with increased collagen deposition, as also noted by Wang *et al*. and Ge *et al*.[1,41]. This fibrosis is linked to oxidative stress and pro-inflammatory cytokines, which stimulate myofibroblasts and fibrogenic gene expression[39,40].

Hepatotoxicity caused by CCl4 activated Kupffer cells which in turn release different cytokines and chemokines. These cytokines activate neutrophils and promote their migration into the hepatic vasculature. When neutrophils were chemotactically activated, they adhere to liver cells inducing cell necrosis and death through the release of reactive oxygen species (ROS) and proteases[42].

Rats treated with 1×10^6 BM-MSCs (Subgroup IIB) revealed a significant improvement in liver structure in comparison with the CCl4 group (Subgroup IIA). Histological and electron microscopy analysis revealed restoration of hepatocyte ultrastructure, with increased mitochondria and minimal inflammatory infiltration, similar to the findings of Feng *et al*. and Elzainy *et al*. They reported normal hepatocytes with few cells with slight vacuolated cytoplasm. Portal tracts were normal with some mildly dilated portal venules and few periportal inflammatory cells[43,44]. Elzainy explained that BM-MSCs can reduce oxidative stress mainly by increasing the activity of antioxidant enzymes[44].

Also, BM-MSCs promote liver repair by secreting Metalloproteinases (MMP1, MMP9), which remodel the extracellular matrix and reduce inflammation and fibrosis[26,45]. Luan *et al*., added that another role of BM-MSC in liver fibrosis recovery by inducing regeneration of liver stem cells via hepatocyte growth factor[46].

Masson trichrome staining showed reduced collagen deposition in the BM-MSCs group, with results similar to Liu *et al*. and Tian *et al*.[22,39], indicating decreased fibrosis. A significant decrease in TNF-α expression in subgroup IIB supports the role of BM-MSCs in modulating inflammation, in agreement with Luo *et al*.[47]. Liver function tests showed improved AST, ALT, total bilirubin, and direct bilirubin levels in BM-MSCs group, aligning with Feng *et al*. and Elzainy *et al*.[43,44].

Prostaglandin E2 (PGE2), TGF-β, and nitric oxide are soluble substances secreted by BM-MSCs that prevent T cell activation and encourage proinflammatory cells to differentiate into regulatory T cells[48]. They also convert M1 macrophages to M2 macrophages and alleviate fibrosis by releasing matrix metalloproteinases (MMPs) and reducing tissue inhibitors of metalloproteinas-1TIMP-1 levels[49].

Wang *et al*. linked MSC benefits to hepatocyte-like cell differentiation, regulation of lipid metabolism, and reduced oxidative stress[50]. Tian *et al*. highlighted that BM-MSCs exert therapeutic effects through paracrine mechanisms and exosomes, promoting liver regeneration and reducing fibrosis, while Elzainy *et al*. emphasized the effect of MSC bioactive mediators in modulating inflammation and stimulating progenitor cell proliferation[22].

The study showed that BM-MSCs-derived exosomes (BM-MSCs-EXOs) were more effective than BM-MSCs in alleviating liver fibrosis. H&E staining of liver tissue in the exosome-treated group (Subgroup IIC) showed significant improvement, with near-normal hepatocytes, minor inflammatory infiltration, and restored liver architecture, similar to the findings of Rong *et al*. and Ma *et al*.[21,51]. Electron microscopy revealed restored ultrastructure in hepatocytes, including mitochondria, rER, glycogen granules, and microvilli, matching the control group's structure.

Masson's trichrome staining revealed collagen deposition reduction in the BM-MSCs-EXO-treated group comparing by both the CCl4 and BM-MSCs-treated groups. The results agreed with Rong *et al*. and Ma *et al*.[21,51], who noted that circCDK13 and miR-17-5p/KAT2B, BM-MSCs-EXOs prevent the activation of HSCs and decrease inflammatory mediators like TNF-α, IL-1, and IL-6. They modulate immune responses, shifting macrophages to M2 which is an anti-inflammatory phenotype[52,53]. Additionally, exosomes promoted the expression of MMPs and anti-inflammatory cytokines, while reducing collagen production, as noted by Bruno *et al*.[54].

Moreover, Chen *et al*. found that exosomes can reduce hepatocyte apoptosis, suppress the inflammatory reaction in the injured liver, and reduce the production of proinflammatory mediators (IL-2, IL-6, IL-10, IL-12p70, interferon-gamma, and TNF-α)[55].

Liver function tests revealed significant improvement in the BM-MSCs-EXO-treated group, including reductions in ALT, AST, total bilirubin, and direct bilirubin, and increased albumin levels, similar to reports by Rong *et al*. and Tian *et al*. They found that BM-MSCs mainly make their impact by paracrine mechanisms of exosomes. They added that BM-MSCs-EXOs have therapeutic properties, like alleviating inflammation and fibrosis, encouraging liver cell regeneration, and improving their performance[21,22].

BM-MSCs-EXOs were found to be as effective as BM-MSCs in promoting liver repair, with advantages including smaller size, easier production, no risk of tumor formation, and lower immunogenicity. These properties make BM-MSCs-EXOs a safer and more efficient option for liver regeneration, as confirmed by Rong *et al*.[21].

CONCLUSION

To summarize, the results of the recent study support the idea that both BM-MSCs and their exosomes have significant potential in treating liver fibrosis, with

exosomes emerging as a promising alternative to whole-cell therapies because they have lower immunogenicity and practical advantages. These findings open the door for future clinical investigations focused on optimizing exosome-based therapies for liver diseases, potentially offering a safer, more effective, and easily administered option for patients suffering from chronic liver conditions like fibrosis and cirrhosis.

CONFLICT OF INTERESTS

There are no conflicts of interest.

REFERENCES

1. Wang R, Song F, Li S, Wu B, Gu Y, Yuan Y. Salvianolic acid A attenuates CCl4-induced liver fibrosis by regulating the PI3K/AKT/mTOR, Bcl-2/Bax and caspase-3/cleaved caspase-3 signaling pathways. Drug design, development and therapy. 2019 May 31:1889-900. https://doi.org/10.2147/DDDT.S194787
2. Roehlen N, Crouchet E, Baumert TF. Liver fibrosis: mechanistic concepts and therapeutic perspectives. Cells. 2020 Apr 3;9(4):875. https://doi.org/10.3390/cells9040875
3. Chen G, Weiskirchen S, Weiskirchen R. Vitamin A: too good to be bad?. Frontiers in Pharmacology. 2023 May 22;14:1186336. https://doi.org/10.3389/fphar.2023.1186336
4. Xie S, Qi H, Li Q, Zhang K, Zhang L, Cheng Y, Shen W. Liver injury monitoring, fibrosis staging and inflammation grading using T1rho magnetic resonance imaging: an experimental study in rats with carbon tetrachloride intoxication. BMC gastroenterology. 2020 Dec;20:1-0. https://doi.org/10.1186/s12876-020-1161-3
5. Datsko VA, Fedoniuk LY, Ivankiv YI, Kurylo KI, Volska AS, Malanchuk SL, Oleshchuk OM. Experimental cirrhosis: liver morphology and function. Wiad Lek. 2020 Jan 1;73(5):947-52. Doi: 10.36740, wlek202005120
6. Novo E, Bocca C, Foglia B, Protopapa F, Maggiora M, Parola M, Cannito S. Liver fibrogenesis: un update on established and emerging basic concepts. Archives of Biochemistry and Biophysics. 2020 Aug 15;689:108445. https://doi.org/10.1016/j.abb.2020.108445
7. Tang P, Jiang W, Lyu S, Brusseau ML, Xue Y, Qiu Z, Sui Q. Mechanism of carbon tetrachloride reduction in ferrous ion activated calcium peroxide system in the presence of methanol. Chemical Engineering Journal. 2019 Apr 15;362:243-50. https://doi.org/10.1016/j.cej.2019.01.034
8. Abd-Elhakim YM, Ghoneim MH, Ebraheim LL, Imam TS. Taurine and hesperidin rescues carbon tetrachloride-triggered testicular and kidney damage in rats via modulating oxidative stress and inflammation. Life Sciences. 2020 Aug 1;254:117782. https://doi.org/10.1016/j.lfs.2020.117782
9. Unsal V, Cicek M, Sabancilar I. Toxicity of carbon tetrachloride, free radicals and role of antioxidants. Reviews on environmental health. 2020 Jun 25;36(2):279-95. https://doi.org/10.1515/reveh-2020-0048
10. Guven A, Nur G, Deveci HA. Biochemical and histopathological profile of the liver in chemical poisoning. Oxidative Stress and Antioxidant Defense System. 2021 Sep 15:123. https://books.google.com.eg/books?id=SM6TEAAAQBAJ
11. Baogui XU, Zheng J, Xiaoxiao TI, Falei YU, Zhongliang LI, Zuisu YA, Xianjun DI. Antihepatofibrotic effect of Guizhifuling pill (桂枝茯苓丸) on carbon tetrachloride-induced liver fibrosis in mice. Journal of Traditional Chinese Medicine. 2022 Oct 10;42(5):715. https://doi.org/10.19852/j.cnki.jtcm.20220707.003
12. Pittenger MF, Discher DE, Péault BM, Phinney DG, Hare JM, Caplan AI. Mesenchymal stem cell perspective: cell biology to clinical progress. NPJ Regenerative medicine. 2019 Dec 2;4(1):22. https://doi.org/10.1038/s41536-019-0083-6
13. Gazit Z, Pelled G, Sheyn D, Yakubovich DC, Gazit D. Mesenchymal stem cells. InPrinciples of regenerative medicine 2019 Jan 1 (pp. 205-218). Academic Press. https://doi.org/10.1016/B978-0-12-809880-6.00014-X
14. Cao Y, Ji C, Lu L. Mesenchymal stem cell therapy for liver fibrosis/cirrhosis. Annals of translational medicine. 2020 Apr;8(8). https://doi.org/10.21037/atm.2020.02.119
15. Gurunathan S, Kang MH, Kim JH. A comprehensive review on factors influences biogenesis, functions, therapeutic and clinical implications of exosomes. International journal of nanomedicine. 2021 Feb 17:1281-312. https://doi.org/10.2147/IJN.S291956
16. Sidhom K, Obi PO, Saleem A. A review of exosomal isolation methods: is size exclusion chromatography the best option?. International journal of molecular sciences. 2020 Sep 4;21(18):6466. https://doi.org/10.3390/ijms21186466
17. Han QF, Li WJ, Hu KS, Gao J, Zhai WL, Yang JH, Zhang SJ. Exosome biogenesis: machinery, regulation, and therapeutic implications in cancer. Molecular cancer. 2022 Nov 1;21(1):207. https://doi.org/10.3390/ijms21186466
18. Zhang F, Zhang L, Yu H. Potential Druggability of Mesenchymal Stem/Stromal Cell-derived Exosomes. Current Stem Cell Research & Therapy. 2024 Oct 1;19(9):1195-209. https://doi.org/10.2174/011574888X311270240319084835
19. Yagi S, Hirata M, Miyachi Y, Uemoto S. Liver regeneration after hepatectomy and partial liver transplantation. International Journal of Molecular Sciences. 2020 Nov 9;21(21):8414. https://doi.org/10.3390/ijms21218414

20. Li W, Li L, Hui L. Cell plasticity in liver regeneration. Trends in cell biology. 2020 Apr 1;30(4):329-38. https://doi.org/10.1016/j.tcb.2020.01.007

21. Rong X, Liu J, Yao X, Jiang T, Wang Y, Xie F. Human bone marrow mesenchymal stem cells-derived exosomes alleviate liver fibrosis through the Wnt/β-catenin pathway. Stem cell research & therapy. 2019 Dec;10:1-1. https://doi.org/10.1186/s13287-019-1204-2

22. Tian S, Zhou X, Zhang M, Cui L, Li B, Liu Y, Su R, Sun K, Hu Y, Yang F, Xuan G. Mesenchymal stem cell-derived exosomes protect against liver fibrosis via delivering miR-148a to target KLF6/STAT3 pathway in macrophages. Stem cell research & therapy. 2022 Jul 20;13(1):330. https://doi.org/10.1186/s13287-022-03010-y

23. Drommelschmidt K, Serdar M, Bendix I, Herz J, Bertling F, Prager S, Keller M, Ludwig AK, Duhan V, Radtke S, De Miroschedji K. Mesenchymal stem cell-derived extracellular vesicles ameliorate inflammation-induced preterm brain injury. Brain, behavior, and immunity. 2017 Feb 1;60:220-32. https://doi.org/10.1016/j.bbi.2016.11.011

24. Khalil MR, El-Demerdash RS, Elminshawy HH, Mehanna ET, Mesbah NM, Abo-Elmatty DM. Therapeutic effect of bone marrow mesenchymal stem cells in a rat model of carbon tetrachloride induced liver fibrosis. Biomedical journal. 2021 Oct 1;44(5):598-610. https://doi.org/10.1016/j.bj.2020.04.011

25. Zhang J, Rong Y, Luo C, Cui W. Bone marrow mesenchymal stem cell-derived exosomes prevent osteoarthritis by regulating synovial macrophage polarization. Aging (Albany NY). 2020 Dec 12;12(24):25138. https://doi.org/10.18632/aging.104110

26. Chu DT, Phuong TN, Tien NL, Tran DK, Thanh VV, Quang TL, Truong DT, Pham VH, Ngoc VT, Chu-Dinh T, Kushekhar K. An update on the progress of isolation, culture, storage, and clinical application of human bone marrow mesenchymal stem/stromal cells. International journal of molecular sciences. 2020 Jan 21;21(3):708. https://doi.org/10.3390/ijms21030708

27. Alzhrani GN, Alanazi ST, Alsharif SY, Albalawi AM, Alsharif AA, Abdel-Maksoud MS, Elsherbiny N. Exosomes: Isolation, characterization, and biomedical applications. Cell Biology International. 2021 Sep;45(9):1807-31. https://doi.org/10.1002/cbin.11620

28. Goldring JD. Measuring protein concentration with absorbance, Lowry, Bradford Coomassie blue, or the Smith bicinchoninic acid assay before electrophoresis. Electrophoretic Separation of Proteins: Methods and Protocols. 2019:31-9. https://doi.org/10.1007/978-1-4939-8793-1_3

29. Habibian A, Soleimanjahi H, Hashemi SM, Babashah S. Characterization and comparison of mesenchymal stem cell-derived exosome isolation methods using culture supernatant. Archives of Razi Institute. 2022 Aug 31;77(4):1383. https://doi.org/10.22092/ARI.2021.356141.1790

30. El-Kashef DH, Abdelrahman RS. Montelukast ameliorates Concanavalin A-induced autoimmune hepatitis in mice via inhibiting TNF-α/JNK signaling pathway. Toxicology and Applied Pharmacology. 2020 Apr 15;393:114931. https://doi.org/10.1016/j.taap.2020.114931

31. Ozevren H, Cetin A, Baloglu M, Deveci E. Evaluation of the association between biochemical and immunohistochemical score of caspase-9 and TNFα, and the grading of lumbar disc herniation. British Journal of Neurosurgery. 2021 Nov 2;35(6):770-4. https://doi.org/10.1080/02688697.2020.1817314

32. Ayala-Lopez N, Conklin SE, Tenney BJ, Ness M, Marzinke MA. Comparative evaluation of blood collection tubes for clinical chemistry analysis. Clinica Chimica Acta. 2021 Sep 1;520:118-25. https://doi.org/10.1016/j.cca.2021.05.019

33. Shakya AK. Drug-induced hepatotoxicity and hepatoprotective medicinal plants: a review. Indian J Pharm Educ Res. 2020 Apr 1;54(2):234-50. DOI: 10.5530/ijper.54.2.28

34. Wu BM, Liu JD, Li YH, Li J. Margatoxin mitigates CCl4-induced hepatic fibrosis in mice via macrophage polarization, cytokine secretion and STAT signaling. International Journal of Molecular Medicine. 2020 Jan;45(1):103-14. https://doi.org/10.3892/ijmm.2019.4395

35. Zein N, Yassin F, Makled S, Alotaibi SS, Albogami SM, Mostafa-Hedeab G, Batiha GE, Elewa YH. Oral supplementation of policosanol alleviates carbon tetrachloride-induced liver fibrosis in rats. Biomedicine & Pharmacotherapy. 2022 Jun 1;150:113020. https://doi.org/10.1016/j.biopha.2022.113020

36. Hassan NF, Soliman GM, Okasha EF, Shalaby AM. Histological, immunohistochemical, and biochemical study of experimentally induced fatty liver in adult male albino rat and the possible protective role of pomegranate. Journal of Microscopy and Ultrastructure. 2018 Jan 1;6(1):44-55. https://doi.org/10.4103/JMAU.JMAU_5_18

37. Li R, Zhang P, Li C, Yang W, Yin Y, Tao K. Tert-butylhydroquinone mitigates carbon tetrachloride induced hepatic injury in mice. International journal of medical sciences. 2020;17(14):2095. https://doi.org/10.7150/ijms.45842

38. Salem BA, ElKaliny HH, Abd El-Hafez AA, Sarhan NI. Comparative Histological Study of Therapeutic Effect of Mesenchymal Stem Cells versus Mesenchymal Stem Cells Co-Cultured with Liver Tissue on Carbon Tetrachloride-Induced Hepatotoxicity in Adult Male Albino Rats. Journal of Microscopy and Ultrastructure. 2022 Nov 2. https://doi.org/10.4103/jmau.jmau_62_21

39. Liu P, Qian Y, Liu X, Zhu X, Zhang X, Lv Y, Xiang J. Immunomodulatory role of mesenchymal stem cell therapy in liver fibrosis. Frontiers in Immunology. 2023 Jan 4;13:1096402. https://doi.org/10.3389/fimmu.2022.1096402

40. Hao Y, Song S, Li T, Zai Q, Ma N, Li Y, Yang L, Xiao P, Xu T, Ji L, Tan J. Oxidative stress promotes liver fibrosis by modulating the microRNA-144 and SIN3A-p38 pathways in hepatic stellate cells. International Journal of Biological Sciences. 2024;20(7):2422. https://doi.org/10.7150/ijbs.92749

41. Ge C, Tan J, Lou D, Zhu L, Zhong Z, Dai X, Sun Y, Kuang Q, Zhao J, Wang L, Liu J. Mulberrin confers protection against hepatic fibrosis by Trim31/Nrf2 signaling. Redox biology. 2022 May 1;51:102274. https://doi.org/10.1016/j.redox.2022.102274

42. Elufioye TO, Habtemariam S. Hepatoprotective effects of rosmarinic acid: Insight into its mechanisms of action. Biomedicine & Pharmacotherapy. 2019 Apr 1;112:108600. https://doi.org/10.1016/j.biopha.2019.108600

43. Feng Y, Li Y, Xu M, Meng H, Dai C, Yao Z, Lin N. Bone marrow mesenchymal stem cells inhibit hepatic fibrosis via the AABR07028795. 2/rno-miR-667-5p axis. Stem Cell Research & Therapy. 2022 Jul 28;13(1):375. https://doi.org/10.1186/s13287-022-03069-7

44. Elzainy A, El Sadik A, Altowayan WM. Comparison between the Regenerative and Therapeutic Impacts of Bone Marrow Mesenchymal Stem Cells and Adipose Mesenchymal Stem Cells Pre-Treated with Melatonin on Liver Fibrosis. Biomolecules. 2024 Mar 1;14(3):297. https://doi.org/10.3390/biom14030297

45. Liu Z, Zhou S, Zhang Y, Zhao M. Rat bone marrow mesenchymal stem cells (BMSCs) inhibit liver fibrosis by activating GSK3β and inhibiting the Wnt3a/β-catenin pathway. Infectious Agents and Cancer. 2022 Apr 19;17(1):17. https://doi.org/10.1186/s13027-022-00432-4

46. Luan Y, Kong X, Feng Y. Mesenchymal stem cells therapy for acute liver failure: recent advances and future perspectives. Liver Research. 2021 Jun 1;5(2):53-61. https://doi.org/10.1016/j.livres.2021.03.003

47. Luo XY, Meng XJ, Cao DC, Wang W, Zhou K, Li L, Guo M, Wang P. Transplantation of bone marrow mesenchymal stromal cells attenuates liver fibrosis in mice by regulating macrophage subtypes. Stem Cell Research & Therapy. 2019 Dec;10:1-1. https://doi.org/10.1186/s13287-018-1122-8

48. Beeken LJ, Ting DS, Sidney LE. Potential of mesenchymal stem cells as topical immunomodulatory cell therapies for ocular surface inflammatory disorders. Stem Cells Translational Medicine. 2021 Jan 1;10(1):39-49. https://doi.org/10.1002/sctm.20-0118

49. Yao Y, Xia Z, Cheng F, Jang Q, He J, Pan C, Zhang L, Ye Y, Wang Y, Chen S, Su D. Human placental mesenchymal stem cells ameliorate liver fibrosis in mice by upregulation of Caveolin1 in hepatic stellate cells. Stem Cell Research & Therapy. 2021 May 20;12(1):294. https://doi.org/10.1186/s13287-021-02358-x

50. Wang C, Zhou H, Wu R, Guo Y, Gong L, Fu K, Ma C, Peng C, Li Y. Mesenchymal stem cell-derived exosomes and non-coding RNAs: regulatory and therapeutic role in liver diseases. Biomedicine & Pharmacotherapy. 2023 Jan 1;157:114040. https://doi.org/10.1016/j.biopha.2022.114040

51. Ma J, Li Y, Chen M, Wang W, Zhao Q, He B, Zhang M, Jiang Y. hMSCs-derived exosome circCDK13 inhibits liver fibrosis by regulating the expression of MFGE8 through miR-17-5p/KAT2B. Cell Biology and Toxicology. 2023 Apr;39(2):1-22. https://doi.org/10.1007/s10565-022-09714-4

52. Lotfy A, AboQuella NM, Wang H. Mesenchymal stromal/stem cell (MSC)-derived exosomes in clinical trials. Stem Cell Research & Therapy. 2023 Apr 7;14(1):66. https://doi.org/10.1186/s13287-023-03287-7

53. Hu X, Ge Q, Zhang Y, Li B, Cheng E, Wang Y, Huang Y. A review of the effect of exosomes from different cells on liver fibrosis. Biomedicine & Pharmacotherapy. 2023 May 1;161:114415. https://doi.org/10.1016/j.biopha.2023.114415

54. Bruno S, Chiabotto G, Camussi G. Extracellular vesicles: a therapeutic option for liver fibrosis. International Journal of Molecular Sciences. 2020 Jun 15;21(12):4255. https://doi.org/10.3390/ijms21124255

55. Chen L, Brenner DA, Kisseleva T. Combatting fibrosis: exosome-based therapies in the regression of liver fibrosis. Hepatology communications. 2019 Feb;3(2):180-92. https://doi.org/10.1002/hep4.1290

الملخص العربى

دراسة نسيجية للدور العلاجي لخلايا النسيج الأوسط الجذعية للنخاع العظمي مقارنة بالإكزوسومات المشتقة منها على تليف الكبد المستحث تجريبياً في ذكر الجرذ الأبيض البالغ

الاء مصطفى قاسم، سارة عبد الجواد، محمد عبد الرحمن، هبه محمد فوزى

قسم الهستولوجى، كلية الطب، جامعة عين شمس

مقدمة: يعد تليف الكبد مشكلة صحية عالمية كبيرة مع خيارات علاج محدودة، باستثناء إزالة السبب الأساسي أو زراعة الكبد. أظهرت الخلايا الجذعية الوسيطة لنخاع العظام والإكزوسومات المشتقة منها إمكاناتها كعوامل علاجية بسبب خصائصها التجديدية والمناعية.

الهدف من العمل: هو مقارنة التأثير العلاجي للخلايا الجذعية الوسيطة لنخاع العظام مقابل الإكزوسومات المشتقة منها على بنية ووظيفة الكبد في تليف الكبد الناجم عن رابع كلوريد الكربون في ذكور الفئران البيضاء البالغة.

المواد والطرق: تم تضمين أربعين من ذكور الفئران البيضاء البالغين في هذه الدراسة. تضمنت المجموعة الأولى (المجموعة الضابطة) عشرة فئران. تلقى ثلاثون فأرا رابع كلوريد الكربون لتحريض تليف الكبد ثم تم تقسيمها بالتساوي إلى المجموعة الثانية أ(مجموعة رابع كلوريد الكربون)، والمجموعة الثانية ب(مجموعة الخلايا الجذعية الوسيطة لنخاع العظام) تلقت الخلايا الجذعية مرة واحدة والمجموعة الثانية ج (مجموعة الإكزوسومات) تلقت إكزوسومات مرة واحدة.

النتائج: تسبب حقن رابع كلوريد الكربون بشكل كبير في حدوث خلل كبدي. تسبب في تبدل نسيجي ملحوظ، كما أكد الهيماتوكسيلين والإيوسين، وفحص المجهر الإلكتروني، والتحليل الكيميائي الحيوي لوظائف الكبد. أظهرت الفئران المعالجة بالخلايا الجذعية الوسيطة لنخاع العظام والإكزوسومات تحسنا كبيرا مقارنة بالمجموعة المعالجة برابع كلوريد الكربون. كان هناك أيضا انخفاض كبير في كل من النسب المئوية للكولاجين وخلايا الكبد الإيجابية لعامل نخر الورم ألفا في هذه المجموعات مقارنة بالمجموعة المعالجة ب رابع كلوريد الكربون. على الرغم من أن الفئران التي عولجت بالإكزوسومات أظهرت تحسنا أكبر في الهيماتوكسيلين والإيوسين والبنية التحتية والتحليل الكيميائي الحيوي، إلا أنه كان هناك اختلاف إحصائي غير كبير بين الخلايا الجذعية الوسيطة لنخاع العظام ومجموعة الإكزوسومات.

الخلاصة: كشفت هذه الدراسة أن التأثير العلاجي للإكزوسومات المشتقة من الخلايا الجذعية الوسيطة لنخاع العظام يبدو أنه قد تم تعزيزه على تأثير الخلايا الجذعية الوسيطة لنخاع العظام نفسها في نموذج لتليف الكبد الناجم عن رابع كلوريد الكربون.